

Experience from measuring the LHC Quadrupole axes

P. Schnizer¹, L. Bottura², G. Deferne², M. Dupont², D. Missiaen², N. Krotov², N. Smirnov²,
P. Winkes²

¹GSI 64291 Darmstadt Germany

²CERN 1211 Geneva 23 Switzerland

Abstract

For historical reasons a pool of equipment is available to measure the axis of the LHC arc quadrupoles. Any of them needs a survey measurement to reference its intrinsic coordinate system to the cryostat fiducials. Up to now 10 quadrupoles have been measured in cold condition. We present our experience, our success next to our failures, explaining the reasons of these failures. This contribution emphasises the day to day problems of such measurements in an "industrial" environment and shows simple aids to circumvent them.

1. INTRODUCTION

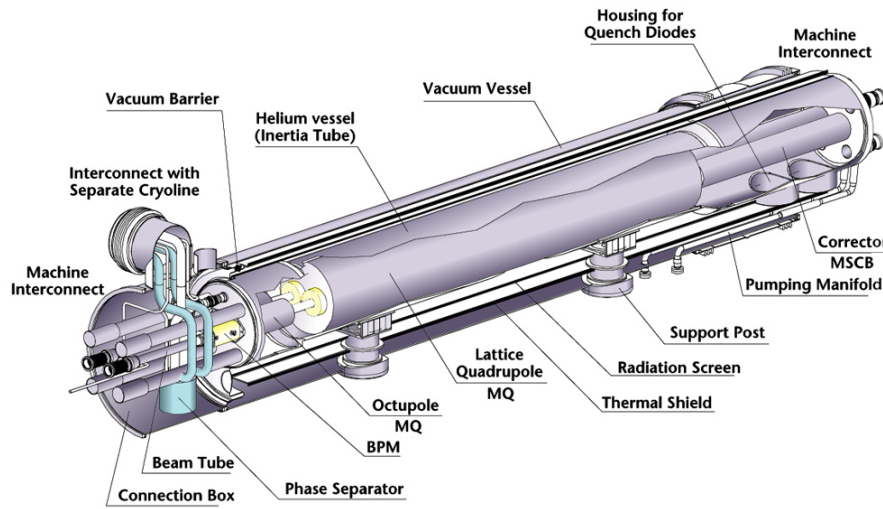
Quadrupoles are the primary focusing elements in an accelerator. If they are not installed perfectly (with a precision of 0.3 mm for the Large Hadron Collider (LHC) at CERN) on the ideal orbit, they will bend the beam off the orbit, like a misplaced conventional lens in an optical system. This paper reviews the techniques applied to the quadrupole measurement, describes the measurement procedure and shows results of the first measured magnets.

The quadrupoles for LHC are installed inside the Short Straight Section (SSS) (see Fig. 1). Many different components are mounted in these magnets [1]. This paper focuses only on the magnetic elements: the main quadrupole (MQ) and its two correctors, the combined dipole sectupole corrector (MSCB) and a octupole (MO) or quadrupole corrector (MQT). Three fiducials are mounted on top of the cryostat. The goal of the axis measurement is to measure the axis with respect to these fiducials in cold and warm condition with a precision of 0.15 mm . These data can be used to install the magnet in the tunnel.

2. MEASUREMENT SYSTEM

Two induction based methods exist to measure the field of a quadrupole. The "automated scanner" uses a rotating coil, and the "Single Stretched Wire" (SSW) a moving wire. Below we describe the two systems.

LHC Short Straight Section



CERN AC_E12-10E

Figure 1. Schematic view of the SSS. This paper focuses on the measurement of the magnets. The main quadrupole is mounted right in the middle. The octupoles are mounted on the left and the combined quadrupole sextupole corrector on the right.

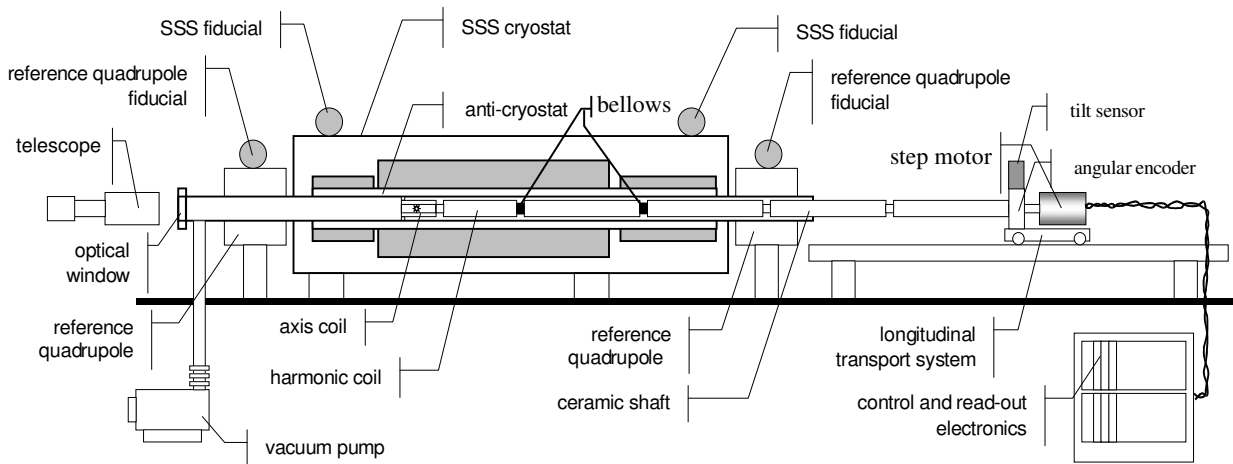


Figure 2. Sketch of the automated scanner system. A anticryostat is placed inside the bore. In this bore a axis searching coil can scan the magnetic fields. A telescope establishes a reference frame inside the bore. The reference quadrupoles are needed to transfer the telescope axis to the fiducials. The anticryostat is evacuated.

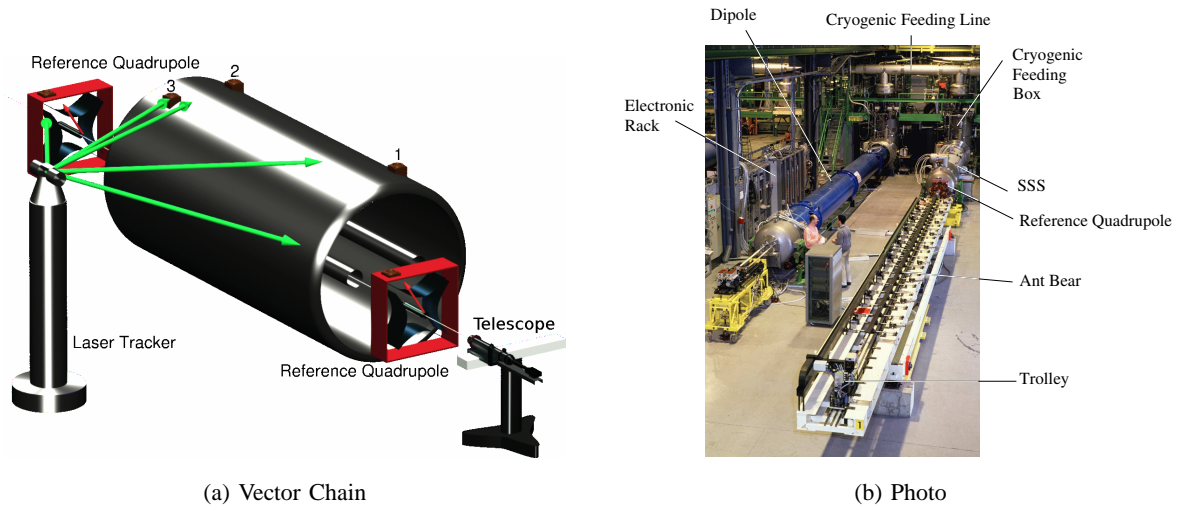


Figure 3. Axis measurement equipment (on the left). The Laser tracker measures the position of the survey targets (green arrows). The reference quadrupole axis is measured with respect to the fiducials. The reference quadrupole's axes offset to the survey target is measured on a dedicated bench (red arrows). The telescope establishes a frame inside the aperture. This frame is transferred to the reference frame using the reference quadrupole axes. The vertical axis of this frame is chosen parallel to gravity. A photo of the setup is given on the right.

2.1 The automated scanner

Originally developed to scan the prototype dipoles, it was adapted to measure the quadrupoles. A more detailed description is found in [2]. Here a rotating coil is used to measure the magnetic field (see Fig. 2). It can be placed at any required longitudinal position, and a telescope is used to establish a reference frame inside the bore (A photo of the setup is given in Fig 3(b)). All magnets have to be scanned to obtain their axes. The steps are outlined in the following (see also Figure 3(a)):

- 1) The axis searching coil (length 100 mm) is placed inside the first reference quadrupole. A magnetic and an optical measurement are performed. Using the voltage of the coil one can derive the offset of the rotation axis from the magnet's field axis; see also Appendix I. This establishes the first point of the telescope reference frame. The vertical axis of this frame is aligned with gravity.
- 2) The axis searching coil is placed inside the MQ with a step rate of 300 mm . At each step a magnetic and an optical measurement are performed. Even without covering the whole magnet, the axis can be measured with good precision by a limited sample of points, as the magnet and anti-cryostat deformation is smooth.
- 3) The axis searching coil is placed inside the second reference quadrupole. A magnetic and an optical measurement are performed delivering the second reference point for the telescope frame.

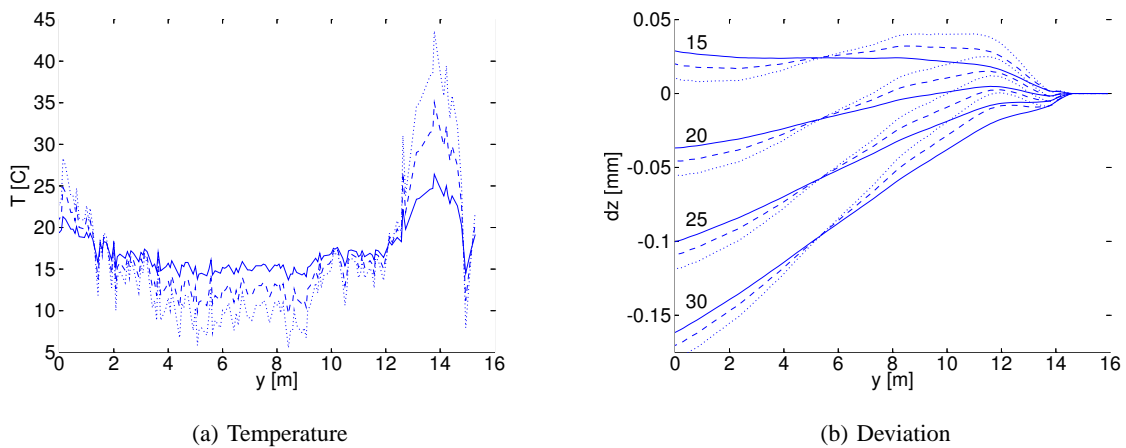


Figure 4. Temperature profile and the resulting beam deviation. The temperature of the anticryostat surface is plotted on the left. The solid line shows the measured temperature. The dotted line was scaled by a factor of two and the dashed line by a factor of three. The result of the ray tracing through the temperature deviation is given on the right. The assumed ambient temperature is given over the ray bundles. The largest deviation is created by the temperature gradient between the ambient air and the air inside the anticryostat.

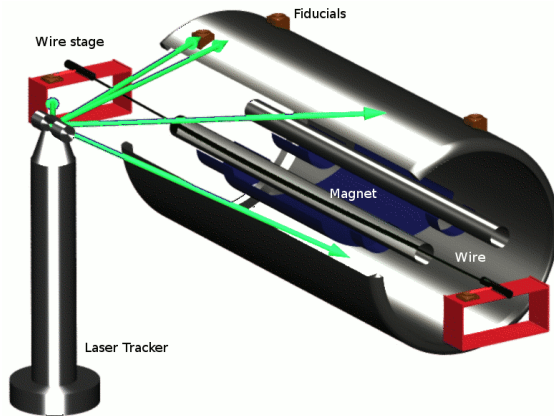
- 4) A survey measurement is performed to measure the position of the reference quadrupoles with respect to the SSS's fiducials. Together with the calibration data of the reference quadrupoles, which measured the distance of the quadrupoles axes to their fiducials, the telescope frame is referred to the SSS's fiducials.

As the magnet is cold, heat is flowing from the anticryostat to the cold magnet lowering the anticryostats inner temperature. Therefore the anticryostat is heated to avoid a constant loss of temperature inside the anticryostat [3]. Early experiments verified [4], [5], [6] that the light is deflected significantly inside the anticryostat.

The code developed in [7] was applied to the temperature profile of the anticryostat [3] (see Fig. 4(a) and Appendix II). For the calculation it was assumed that the temperature difference in y only forms a gradient in z . The temperature profile in Fig. 4(a) was scaled by a factor of two and three to simulate less optimal anticryostats. Different ambient temperatures were chosen: 15, 20, 25 and 30°C. The result of the ray tracing is shown in Fig. 4(b). One can see that the temperature difference between the environment and the anticryostat mainly deviates the beam. Its maximum (0.2 mm) is larger than the acceptable total measurement error. The telescope can measure lateral offsets with a precision of 0.03 mm. Thus it was decided to use glass windows and evacuate the relevant part of the anticryostat.

2.2 The Single Stretched Wire System

The Single Stretched Wire (SSW) [8], [9], [10] is one of the most flexible methods for measuring a magnet. A wire is stretched through the bore (see Fig. 5(a)). When the wire is



(a) Sketch



(b) Stage

Figure 5. The SSW system. Two stages move a wire in both lateral directions. The wire support's calibration is indicated by a red vector (see sketch on the left). A photo of one stage is given on the right.

moved, the magnetic field induces a current in the wire. The system then tries to bring the wire to the quadrupole's axis as close as possible (the integrated voltage is zero if the wire is moving symmetrically with respect to the axis.) Measuring the wire's position (using the support's fiducials) one can calculate the axis with respect to the cryostat fiducials. Contrary to the automated scanner this system can only measure the integrated value of the field.

2.3 The Laser Tracker

A conventional Laser Tracker is used to measure the fiducials of the measurement system (either of the reference quadrupoles of the automated scanner or of the SSW system) with respect to the SSS cryostats fiducials.

3. SCALES OF THE DIFFERENT VECTORS

The measurement involves many different vectors of length widely differing. Table 1 summarises them. They range from less than a millimetre for the magnetic measurement up to a few meters for the survey measurement.

4. RESULTS

4.1 Comparison of the two systems

The systems were first compared in [2] for the prototype SSS 005 with an agreement better than 0.1 mm . In Table 1 the quality of the different components is shown retrieved from dedicated calibration benches for the telescope (Δ_T), the reference quadrupoles (Δ_q), the

Table 1: Typical length and accuracy of the various vectors contributing to the axis. x is horizontal and z vertical. y is the longitudinal component, parallel to the magnet's axis.

name	length		Accuracy $\Delta x, \Delta z [mm]$
	$x, z [mm]$	$y [mm]$	
magnet centre to fiducials	400	1500	0.15
fiducials to tracker	2000	2000	0.05
automated scanner			
axis to coil	1	—	0.01
coil to telescope	3	500 - 15000	0.03
reference quadrupole to fiducials	300	300	0.02
SSW			
axis to wire	1	—	0.02
stage support to fiducials	50	—	0.05

searching coil (Δ_{mag}), and from the specifications for the tracker (Δ_{Lt}). The total accuracy is calculated using

$$\begin{aligned} \Delta_{axis} &= \sqrt{\Delta_q^2 + \Delta_{Lt}^2 + 2(\Delta_T^2 + \Delta_{mag}^2)} \\ &= \sqrt{(20^2 + 50^2 + 2 \cdot (10^2 + 30^2))} \mu m = 70 \mu m \end{aligned} \quad (1)$$

at one standard deviation.

The SSS 001, SSS 004, SSS 002, SSS 013, SSS 015 and SSS 021 were measured with both systems. The fiducials' values were used to transfer the different frames to the same one. The results of the different methods match within $0.2 mm$ for all magnets compared. This value is twice as large as the one obtained during the prototype SSS 005 measurement campaign. The former was performed during the R&D phase in a calm environment, while the later were achieved in a busy measuring hall, in industrial testing conditions. For SSS 002 the results are shown in Fig 6.

4.2 Comparison of warm magnetic and geometric measurements

Beside the described magnetic measurements geometric measurements were performed as well. These match the magnetic measurement data, retrieved when the magnet is warm to $0.1 \pm 0.1 mm$ at one standard deviation (see also Fig 6).

4.3 Cool down effect

The quadrupoles are supported by two feet. These feet shrink during cool down. This distance can be retrieved comparing the cold and warm axis measurement. The data for the first ten SSS

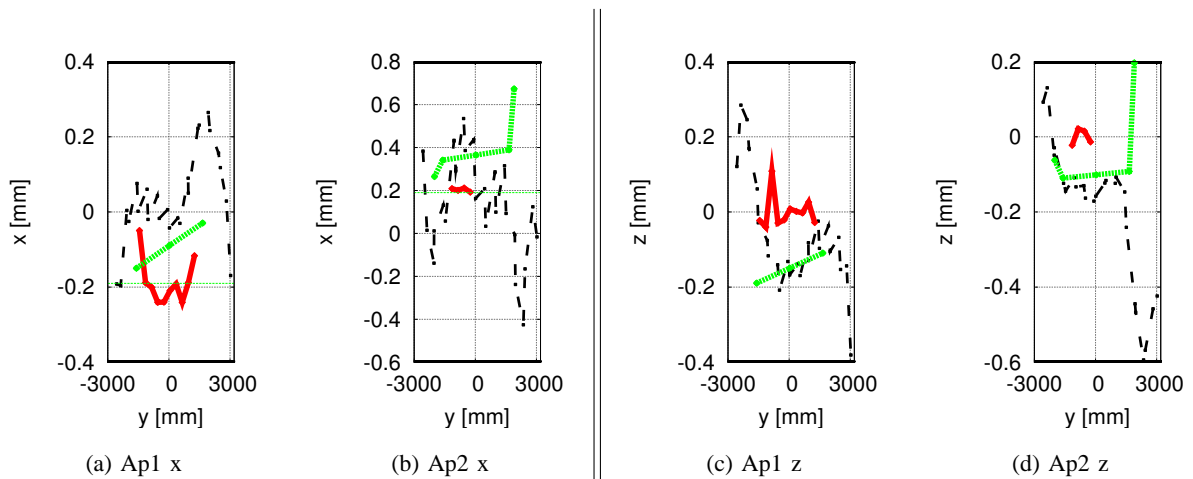


Figure 6. Comparison of the automated scanner, SSW and pure geometrical measurements (reference system). x denotes lateral offsets and z vertical offsets. y is the longitudinal component. The solid line denotes the automated scanner measurements, the dotted line the SSW measurement and the dash dotted one the geometry measurement.

Table 2: Cool down effect as measured for the first ten SSS.

Ap1	x	-0.22	-0.19	-0.09	-0.08	-0.14	-0.05	-0.16	0.75	-0.07	0.11
	z	-1.25	-1.34	-1.31	-1.29	-1.04	-1.06	-1.35	-1.74	-1.31	-1.40
Ap2	x	-0.13	-0.26	0.05	-0.07	-0.35	-0.04	-0.18	-0.11	-0.02	0.13
	z	-1.23	-1.31	-1.33	-1.35	-1.30	-1.43	-1.35	-1.36	-1.19	-1.48

are given in Tab 2. It is $-1.3 \pm 0.2 \text{ mm}$ for Aperture #1 and $-1.3 \pm 0.1 \text{ mm}$ for Aperture #2. For x the standard deviation is 0.3 mm . No significant horizontal movement can be seen.

5. OPERATING EXPERIENCE

As 360 Arc SSS have to be measured along with ≈ 1200 dipoles and ≈ 100 special SSS one always tries to diminish the time needed for measurements even if the measurement time is short compared to the total duration of the cold test. (48 hours of measurement compared to 120 hours on the bench.)

The automated scanner has to scan the magnet, which means, the coil has to be placed successional on different positions, and only then the measurement can be executed, resulting in a time consuming measurement. Further the measurement bench and reference quadrupoles have to be moved from one aperture to the other during the test. In contrary the SSW measures the integral of the axis at once, and is a much faster method. The automated scanner consumes a total of 12 hours for one axis measurement in contrast to the 3 hours needed for the SSW. Thus the SSW system is now favoured for all quadrupoles axis measurements.

As the survey measurement has to be performed over the largest distances it is associated with most troubles. In the beginning it was conducted by the magnetic measurement team

(including PS) and failed during unfavourable conditions: measurement time too long (12 hours measurement time in one go for one axis using the automated scanner); big temperature gradients distorting the survey measurement when the hall doors were left open in winter, unstable conditions in the hall, due to magnets being lifted and transported (≈ 35 metric tons). The survey group has taken over these measurements and since then no major incidents occurred.

The analysis of the axis measurement nowadays needs a somehow sophisticated code dealing with calculations of various different subjects as there are: axis measured by magnetic measurement equipment; combination of point sets; various 3D fitting. Even if for geodesic applications various commercial applications and (perhaps libraries) are around, the codes applied here had to be developed in house, as they had to be closely combined to our other tools, thus lengthening the development of the analysis code.

6. POSSIBLE IMPROVEMENTS

Magnetic measurement experts should search contact to Geodesy experts as soon as possible in the R&D stage for magnet axis measurement systems. Many simple solutions and error reducing strategies already exist for common day to day problem. It is much simpler to install a reference network when not all space is already occupied by different devices, and one can still demand straight lines of sight to be left open. During the R&D phase the contact to our geodesic experts was not as close as it could have been. This resulted in our network being squeezed between the measurement benches. No means were installed to establish a reference for the SSW or telescope frame. Therefore the axis measurement's intermediate steps checks are rather limited as the aforementioned frames are arbitrary. It is common practice in survey measurement series to measure against reference windows (i.e. the measurement software checks if the last measurement fitted to the expected range). This technique was not thought of by the magnet measurement people and therefore it was not implemented.

Even if various commercial applications and (perhaps libraries) are around for geodesic tasks, we would like to call for a free implementation for "simple" geodesic task as there are: "simple" fitting of data sets, simple axis alignments (3 points; axis, point; point, axis, gravity). All these calculations are needed for magnetic axis calculation, but must be closely combined with the pure magnetic measurement treatment. If such codes exists please publish them also on common free software meeting points e.g. <http://sourceforge.net> or <http://savannah.gnu.org/>.

7. CONCLUSION

This paper described the different systems available for the measurement of the quadrupole axis. It was shown that the SSW and the automated scanner produce data which match with a precision of 0.2 mm . Day to day experience showed that the survey measurement is the one with the highest risk as it has to cover the largest measurement space.

8. ACKNOWLEDGEMENT

The authors would like to thank all people supporting the infrastructure in SM 18 and in Bld. 30; all the operators performing the test and data preparation. Special thanks to Patrick Kowalzik for help on developing the Helmert Transform code. Thanks also to Fermi National Laboratory and in particular to J. DiMarco for supplying the SSW system.

Appendix I MAGNETIC AXIS MEASUREMENT WITH A ROTATING COIL

The final aim of a rotating coil system is to measure the field of a magnet and to describe its multipoles C_n . The magnetic field B of accelerator magnets can be expanded in a series as follows:

$$B(z) = B_y + iB_x = \sum_{n=1}^{\infty} [B_n + iA_n] \left(\frac{z}{R_{Ref}} \right)^n \quad (2)$$

where $B_n + iA_n = C_n$ are the multipole components [11], and z the transverse position. The flux Φ seen by a rotating coil is given by [12]:

$$\Phi(t) = \sum_{n=1}^M K_n C_n \cos [n\beta(t)]. \quad (3)$$

M is the highest harmonic taken into account, β is the angular position and K_n the coils sensitivity to the n^{th} harmonic given by:

$$K_n = \left(\frac{N_w L R_{Ref}}{n} \right) \left[\left(\frac{z_2}{R_{Ref}} \right)^n - \left(\frac{z_1}{R_{Ref}} \right)^n \right] \quad (4)$$

where N_w is the number of windings, L the length and z_2 and z_1 the inner and outer radii respectively of the coil. R_{Ref} is the reference radius (for LHC 17 mm). The voltage $V(t)$ induced in the coil is given by:

$$V(t) = -n \dot{\beta}(t) \sum_{n=1}^N K_n C_n \sin [n\beta(t)]. \quad (5)$$

Equation (5) is obtained applying the induction law on (3) assuming a magnetic field which is constant in time. The systems used for the magnetic measurements at CERN is based on digital integrators. The C_n 's are obtained as measurements:

$$C_n = \frac{1}{K_n} FT \left(\int_0^P V(t') dt' \right). \quad (6)$$

where FT denotes the Fourier transform, P the time needed for one revolution of the coil.

The offset z_o of the magnetic axis from the coordinate centre is given by

$$z_o = -\frac{1}{R_{Ref}} \frac{C_{n-1}}{C_n}, \quad (7)$$

with n the main harmonic of the magnet.

Appendix II LIGHT DEFLECTION IN AIR GRADIENTS

The path of light in inhomogeneous media is described by the Eikonal equation[13]

$$\ddot{s} \left(n \frac{d\vec{r}}{ds} \right) = \nabla s, \quad (8)$$

with s the path of the light, r the unity vector or the light's direction. In Cartesian coordinets x, y, z the equations can be written as

$$\frac{d^2 x}{ds^2} = \frac{dn}{dx} - \underbrace{\left(\frac{dn}{dx} \frac{dx}{ds} + \frac{dn}{dy} \frac{dy}{ds} + \frac{dn}{dz} \frac{dz}{ds} \right)}_{corr} \frac{dx}{ds} \quad (9)$$

⋮

For gases one can link the refractivity to the temperature. The refractivity index n is given by[13]

$$n^2 - 1 = 4N\pi\alpha \quad (10)$$

in the CGSM system with α the polarisability and N the number of particles. The ideal gas equation is given by

$$p = NkT, \quad (11)$$

with k the Boltzman konstant, N the number of particles and T the temperature. As the refractivity index of gases is close to 1

$$n^2 - 1 \approx 2(n - 1). \quad (12)$$

Using (11) and (12) n is given by

$$n - 1 = 2\pi\alpha \frac{p}{kT}. \quad (13)$$

For small gradients the term marked *corr* in equation (10) can be neglected and one can derive the approximation

$$\delta z = 10^{-6} \frac{\delta T}{\delta y}. \quad (14)$$

with δz the deviation form the straight line, and $\delta T/\delta y$ the gradient along the light's path.

References

- [1] J. B. Bergot *et al.*, "A modular design for the 56 variants of the Short Straight Section in the arcs of the Large Hadron Collider(LHC)," in *7th European Particle Accelerator Conference, Vienna, Austria, 26 - 30 Jun 2000*. European Phys. Soc., Geneva, 2000, pp. 2157–2163.
- [2] P. Schnizer, "Measuring System Qualification for LHC Arc Quadrupole Magnets (CERN-THESIS-2003-006)," Ph.D. dissertation, Technische Universität Graz, Rechbauerstraße 12, A-8010 Graz, October 2002.
- [3] O. Dunkel, P. Legrand, and P. Sievers, "A Warm Bore Anticyostat for Series Magnetic Measurements of LHC Superconducting Dipole and Short Straight Section Magnets," in *2003 Cryogenic Engineering Conference and International Cryogenic Materials Conference*, Anchorage, AK, USA, 9 2003.
- [4] —, "Private communication," October 1999.
- [5] E. Ainardi, L. Bottura, and N. Smirnov, "Optical and magnetic measurement of quadrupole axis in the cold mass of the saclay-q2 main quadrupole prototype," CERN LHC-MTA, Tech. Rep., 1998.
- [6] —, "Light beam deflection through a 10 m long dipole model," CERN LHC-MTA, Tech. Rep., May 1999.
- [7] P. Schnizer, "Untersuchung des Gaslinsen Effekts in einem Opazimeter." Master's thesis, Technische Universität Graz, Rechbauerstraße 12, A-8010 Graz, 1999.
- [8] J. DiMarco *et al.*, "Field Alignment of Quadrupole Magnets for the LHC Interaction Regions," in *16th Internatiaonal Conference on Magnet Technology (MT-16 1999), Tallahassee, FL, 26 Sept.-2 Oct. 1999*.
- [9] J. DiMarco and J. Krzywinski, "MTF single stretched wire system," Fermi National Accelerator Laberatory, P.O. Box 500, Batavia, Illinois 60510, Tech. Rep., March 1996.
- [10] J. DiMarco *et al.*, "Alignment of production quadrupole magnets for the LHC interaction regions," *IEEE Trans. Appl. Supercond.*, vol. 13, pp. 1325–1328, 2003.
- [11] A. K. Jain, "Basic theory of magnets," in *CAS Magnetic Measurement and Alignment*, S. Turner, Ed. CERN, August 1998, pp. 1–21.
- [12] —, "Harmonic coils," in *CAS Magnetic Measurement and Alignment*, S. Turner, Ed. CERN, August 1998, pp. 175–217.
- [13] B. Born and E. Wolf, *Principles of Optics*, 6th ed. Pergamon Press, 1980.